Characterization of the Class IV Homeodomain-Leucine Zipper Gene Family in Arabidopsis[1][W]

Miyuki Nakamura[2], Hiroshi Katsumata, Mitsutomo Abe[3], Naoto Yabe, Yoshibumi Komeda, Kotaro T. Yamamoto, and Taku Takahashi*

Division of Biological Sciences, Graduate School of Science, Hokkaido University, Sapporo 060–0810, Japan (M.N., H.K., M.A., K.T.Y.); Department of Biological Sciences, Graduate School of Science, The University of Tokyo, Tokyo 113–0033, Japan (N.Y., Y.K.); and Division of Bioscience, Graduate School of Natural Science and Technology, Okayama University, Okayama 700–8530, Japan (T.T.)

The Arabidopsis (*Arabidopsis thaliana*) genome contains 16 genes belonging to the class IV homeodomain-Leucine zipper gene family. These include *GLABRA2*, *ANTHOCYANINLESS2*, *FWA*, *ARABIDOPSIS THALIANA MERISTEM LAYER1* (*ATML1*), and *PROTODERMAL FACTOR2* (*PDF2*). Our previous study revealed that *atml1 pdf2* double mutants have severe defects in the shoot epidermal cell differentiation. Here, we have characterized additional members of this gene family, which we designated *HOMEODOMAIN GLABROUS1* (*HDG1*) through *HDG12*. Analyses of transgenic Arabidopsis plants carrying the gene-specific promoter fused to the bacterial β-glucuronidase reporter gene revealed that some of the promoters have high activities in the epidermal layer of the shoot apical meristem and developing shoot organs, while others are temporarily active during reproductive organ development. Expression profiles of highly conserved paralogous gene pairs within the family were found to be not necessarily overlapping. Analyses of T-DNA insertion mutants of these *HDG* genes revealed that all mutants except *hdg11* alleles exhibit no abnormal phenotypes. *hdg11* mutants show excess branching of the trichome. This phenotype is enhanced in *hdg11 hdg12* double mutants. Double mutants were constructed for other paralogous gene pairs and genes within the same subfamily. However, novel phenotypes were observed only for *hdg3 atml1* and *hdg3 pdf2* mutants that both exhibited defects in cotyledon development. These observations suggest that some of the class IV homeodomain-Leucine zipper members act redundantly with other members of the family during various aspects of cell differentiation. DNA-binding sites were determined for two of the family members using polymerase chain reaction-assisted DNA selection from random oligonucleotides with their recombinant proteins. The binding sites were found to be similar to those previously identified for ATML1 and PDF2, which correspond to the pseudopalindromic sequence 5′-GCATTAAATGC-3′ as the preferential binding site.

Homeodomain-Leu zipper (HD-ZIP) proteins, which are characterized by a HD followed by a ZIP motif (Ruberti et al., 1991), constitute a large family of transcription factors unique to plants. In Arabidopsis (*Arabidopsis thaliana*), the HD-ZIP genes have been classified into four classes (Sessa et al., 1998). Class I consists of 17 members, some of which may act in abscisic acid and Suc signaling pathways, whereas the class II comprises 9 members, some of which have been implicated in phytochrome-mediated shoot morphogenesis (Henriksson et al., 2005, and refs. therein). The well-characterized class III includes five members that function in regulating vascular differentiation, lateral organ polarity, and meristem initiation (Prigge et al., 2005).

The class IV HD-ZIP family is also known as HD-GL2 after the first identified gene *GLABRA2* (*GL2*). Analyses of *gl2* mutants revealed that the *GL2* gene is necessary for both root hairless cell specification and the local outgrowth of the trichome in shoot epidermal cells (Hülskamp et al., 1994; Rerie et al., 1994; Di Cristina et al., 1996; Masucci et al., 1996). The HD-ZIP IV family also includes *ANTHOCYANINLESS2* (*ANL2*), *FWA*, *ARABIDOPSIS THALIANA MERISTEM LAYER1* (*ATML1*), and *PROTODERMAL FACTOR2* (*PDF2*). *anl2* mutants accumulate reduced levels of anthocyanin in subepidermal and epidermal cells in the shoot and have several extra cells between the epidermal and cortical layers in the root (Kubo et al., 1999). The *FWA* gene was identified from a dominant late-flowering mutant with ectopic *FWA* expression that is attributed to epigenetic hypomethylation around its transcription start site (Soppe et al., 2000). *FWA* has been shown to be an imprinted gene (Kinoshita et al.,

[1] This work was supported by a Grant-in-Aid for Scientific Research on Priority Areas (15031201, 17027021 to T.T.) from the Ministry of Education, Culture, Sports, Science, and Technology of Japan.

[2] Present address: Department of Integrated Genetics, National Institute of Genetics, Mishima, Shizuoka 411–8540, Japan.

[3] Present address: Department of Botany, Graduate School of Science, Kyoto University, Kyoto 606–8502, Japan.

* Corresponding author; e-mail perfect@cc.okayama-u.ac.jp; fax 81–86–251–7876.

The author responsible for distribution of materials integral to the findings presented in this article in accordance with the policy described in the Instructions for Authors (www.plantphysiol.org) is: Taku Takahashi (perfect@cc.okayama-u.ac.jp).

[W] The online version of this article contains Web-only data.

Article, publication date, and citation information can be found at www.plantphysiol.org/cgi/doi/10.1104/pp.106.077388.

2004). *ATML1* and *PDF2* are expressed mainly in the protoderm of developing embryos and the outermost layer (L1) of shoot apical meristems (Lu et al., 1996; Sessions et al., 1999; Abe et al., 2003). Previously, we showed that the expression of an Arabidopsis L1-specific gene requires an 8-bp cis-regulatory element that we designated the L1 box (Abe et al., 2001), and that both ATML1 and PDF2 can bind to this element in vitro (Abe et al., 2003). Moreover, disruption of both *ATML1* and *PDF2* by T-DNA insertion results in severe defects in the shoot epidermal cell differentiation (Abe et al., 2003). On the other hand, Tavares et al. (2000) have identified an additional six members of the HD-ZIP IV family that were tentatively denoted as *HD-GL2-1* through *HD-GL2-6. HD-GL2-6* was shown later to be identical to *FWA* (Soppe et al., 2000). Further searches of the GenBank database revealed that the Arabidopsis genome contains a total of 16 HD-ZIP IV genes (Abe et al., 2003; Schrick et al., 2004). Members of the HD-ZIP IV family have also been identified from other plant species. These include five *Zea mays Outer Cell Layer* (*ZmOCL*) genes in maize (Ingram et al., 1999, 2000), *Rice Outermost Cell-specific gene1* (*ROC1*; Ito et al., 2002) and *Oryza sativa Transcription Factor1* (*OSTF1*; Yang et al., 2002) in rice, and two *Picea abies Homeobox* (*PaHB*) genes in Norway spruce (Ingouff et al., 2001, 2003), most of which are preferentially expressed in the protoderm and shoot L1 cells. However, to our knowledge, their functions remain unknown.

To better understand the importance of the HD-ZIP IV family in plant development, we conducted a comprehensive study of this family in Arabidopsis. Here, we report the results of reverse transcription (RT)-PCR analyses, promoter-β-glucuronidase (GUS) expression patterns, DNA-binding assays, and the phenotypes of T-DNA insertion mutants of each HD-ZIP IV member that has not been previously characterized.

RESULTS

The Arabidopsis HD-ZIP IV Family Comprises 16 Genes

In accordance with the previous designation (Tavares et al., 2000), we renamed *HD-GL2-1* through *HD-GL2-6* as *HOMEODOMAIN GLABROUS1* (*HDG1*) through *HDG6*, in which *HDG6* is identical to *FWA*, and designated the new gene members as *HDG7* through *HDG12*. The name, the chromosomal locus assigned by the Arabidopsis Genome Initiative sequencing project, and the length of the deduced amino acid sequences of all members of the Arabidopsis HD-ZIP IV family are summarized in Table I.

Figure 1A shows a phylogenetic relationship between all of the members of the Arabidopsis HD-ZIP III and HD-ZIP IV proteins, which was deduced by using the neighbor-joining method (Saitou and Nei, 1987). The Arabidopsis genome contains many putative paralogs that likely arose via segmental chromosome duplication events (Blanc et al., 2000; Vision et al., 2000). The search for such paralogs within the HD-ZIP IV family by the use of the Paralogons in Arabidopsis program (http://wolfe.gen.tcd.i.e./athal/dup) revealed that *HDG1-ANL2*, *HDG2-HDG3*, *HDG4-HDG5*, *FWA/HDG6-HDG7*, *HDG8-HDG9*, *HDG11-HDG12*, and *ATML1-PDF2* form paralogous gene pairs. The tree shown in Figure 1A supports this notion. However, further phylogenetic analyses, comparing the sequences of Arabidopsis HD-ZIP IV proteins with those of other plant species, suggest that the duplication giving rise to *HDG2* and *HDG3* occurred prior to the divergence of gymnosperms and angiosperms (Supplemental Fig. 1). The high homology between *HDG9* and *HDG10* suggests that they were produced in a local gene duplication after a large-scale genome duplication that produced *HDG8* and *HDG9*.

Table I. *HD-ZIP IV genes in Arabidopsis*

Name	Locus Identification	No. of Amino Acid	GenBank Accession No.
HDG1	At3g61150	808	NP_191674
HDG2	At1g05230	721	NP_172015
HDG3	At2g32370	721	NP_180796
HDG4	At4g17710	709	NP_193506
HDG5	At5g46880	820	NP_199499
FWA/HDG6	At4g25530	686	NP_567722
HDG7	At5g52170	682	NP_200030
HDG8	At3g03260	699	NP_186976
HDG9	At5g17320	718	NP_197234
HDG10	At1g34650	708	NP_174724
HDG11	At1g73360	722	NP_177479
HDG12	At1g17920	687	NP_564041
GL2	At1g79840	747	NP_565223
ANL2	At4g00730	802	NP_567183
ATML1	At4g21750	762	NP_193906
PDF2	At4g04890	743	NP_567274

Both the HD-ZIP III and HD-ZIP IV families of proteins are characterized by an amino-terminal HD-ZIP region followed by a region similar to the mammalian StAR-related lipid-transfer (START) domain (Ponting and Aravind, 1999). Moreover, HD-ZIP IV can be distinguished from HD-ZIP III by the conserved HD helix-III region Q(V/I)KFWFQN(R/K)RTQmK (Fig. 1B), and also by the presence of an internal loop within the ZIP motif (Yang et al., 2002). This motif has also been published as the zipper-loop-zipper motif (Schrick et al., 2004). These features appear to be conserved among both the HD-ZIP IV proteins in gymnosperms (Ingouff et al., 2001) and those found in the expressed sequence tag (EST) database of the moss *Physcomitrella patens* (http://moss.nibb.ac.jp/; Fig. 1C).

According to previous reports (Sessions et al., 1999; Soppe et al., 2000; Abe et al., 2003) and the full-length cDNA sequences deposited in GenBank, *ATML1*, *PDF2*, *HDG2*, *HDG3*, and *FWA/HDG6* contain 5′-untranslated exon(s) that are located far upstream of the start codon, and *HDG2* further contains two sites of transcription initiation (Fig. 2). Unlike the HD-ZIP III genes, all of the Arabidopsis HD-ZIP IV genes have

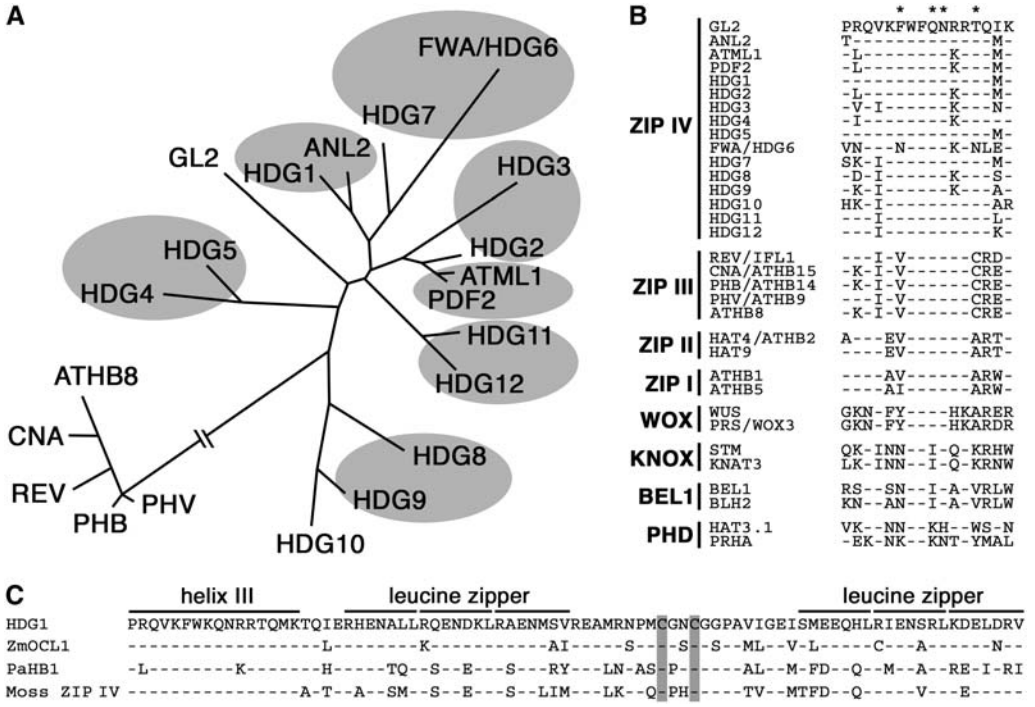

Figure 1. Identity of the Arabidopsis HD-ZIP IV genes. A, Phylogenetic tree showing the predicted relationships between all members of the class III and class IV HD-ZIP proteins of Arabidopsis. Full-length amino acid sequences of each protein were aligned using CLUSTAL W (Thompson et al., 1994) and revised manually. The tree was constructed by using the neighbor-joining method (Saitou and Nei, 1987). Paralogous gene pairs that likely arose via large-scale genome duplications are shaded. B, Sequence comparisons of the HD helix-III region between different classes of the Arabidopsis HD proteins. Two representative members of each family are aligned with all members of HD-ZIP III and IV families. Residues identical to those of GL2 are indicated by dashes. Asterisks denote potential DNA sequence-specific contact residues (Gehring et al., 1994). C, Sequence comparison of the HD helix-III region, followed by the zipper-loop-zipper motif, between the HD-ZIP IV proteins from different plant species. Zm, Pa, and Moss indicate maize, *Picea abies*, and *P. patens*, respectively. Residues identical to those of the Arabidopsis HDG1 are indicated by dashes. Conserved Cyss implicated in redox regulation (Tron et al., 2002) are shaded. GenBank accession numbers are Y17898 (ZmOCL1) and AF172931 (PaHB1). Moss ZIP IV is ASYB17005 in the Physcomitrella EST database (http://moss.nibb.ac.jp/).

a 118-bp exon that encompasses the conserved HD helix-III coding sequence.

HDG7 and 9 Bind to L1 Box-Like Sequences

Previous studies have shown that recombinant ATML1 and PDF2 proteins bind to the L1 box 5′-TAA-ATG(C/T) A-3′ (Abe et al., 2001, 2003). As another approach to identify target sequences of HD-ZIP IV proteins, we selected binding sequences from a pool of random 20-bp DNA fragments by utilizing their recombinant fusions with the maltose-binding protein (MBP). Nearly full-length cDNA sequences of *ATML1*, *HDG7*, and *HDG9* were amplified by RT-PCR and then fused in frame with the MBP sequence of the pMAL vector. After five rounds of the PCR-assisted binding reaction, the selected and amplified DNA fragments were cloned and sequenced. The consensus binding sequences were determined according to the most frequently occurring nucleotides and are summarized in Figure 3. HDG7 showed a binding preference for a pseudopalindromic sequence, 5′-GCATTAAATGC-3′, which partially overlaps with the L1 box. The HDG9 binding sequence 5′-GCATTAAATGCGCA-3′ contains the HDG7 binding sequence and also an L1 box-like motif. The ATML1 binding sequence 5′-CGCAT-TAAATGC-3′ is nearly identical to the HDG7 binding sequence. Significantly, these results are consistent with previous studies demonstrating that the HD-ZIP proteins bind to pseudopalindromic sequences in vitro (Sessa et al., 1993, 1998; Tron et al., 2001). We also determined the PDF2 binding sequence after three rounds of selection and found that its consensus is shorter than the other sequences, probably because there were fewer rounds of selection. MBP alone, which was expressed from the empty pMAL vector as a control, showed no binding preference after five rounds of selection.

Expression Profiles of the Arabidopsis HD-ZIP IV Genes

To compare the expression patterns of all 16 HD-ZIP IV genes, we performed RT-PCR with gene-specific primers (Fig. 4). Each of the primers in these amplifications was designed to distinguish cDNA from

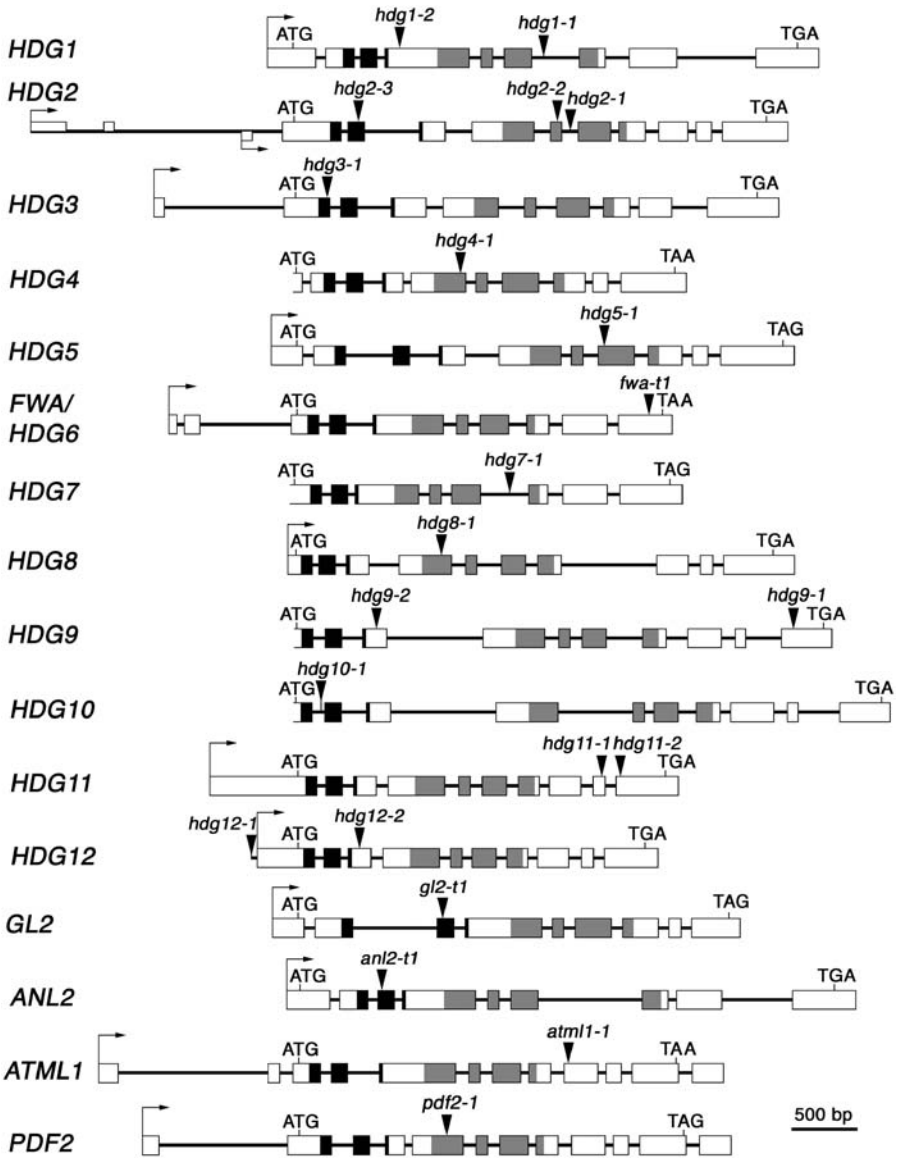

Figure 2. Genomic structures of the Arabidopsis HD-ZIP IV genes and locations of T-DNA insertions. Exons are indicated by boxes, whereas introns are indicated by lines. Black and gray areas represent the regions coding for the HD and the START domain, respectively. Arrowheads indicate the location of the T-DNA insertions. Arrows indicate putative transcription start sites, which are based on the full-length cDNA sequences deposited in GenBank.

genomic DNA by spanning introns (Supplemental Table I). *HDG1*, *HDG2*, *HDG11*, and *HDG12* were expressed in all of the organs analyzed, whereas *HDG3* was expressed only in siliques and seedlings. *HDG5* showed expression in all but the root tissue. *HDG4*, *HDG8*, *HDG9*, and *HDG10* transcripts were detectable after flower organ development. While *FWA*/*HDG6* has been shown to be expressed exclusively in the endosperm (Kinoshita et al., 2004), its paralogous gene, *HDG7*, showed expression only in roots and seedlings. These results indicate that paralogous gene pairs within the HD-ZIP IV family are not necessarily regulated in a common way during development.

Promoter-GUS Expression Patterns of the 11 *HDG* Genes

Spatial and temporal expression patterns of the novel 11 *HDG* genes were further examined by generating the promoter-GUS fusion for each of the genes. Histochemical GUS staining patterns were analyzed in at least four independent transgenic lines for each construct. However, attempts to detect GUS signals in plants with *HDG3* and *HDG4* fusions were unsuccessful.

GUS staining patterns observed in vegetative shoots are shown in Figure 5. The *HDG1* promoter drove GUS expression only in trichomes forming at the base of young leaves (Fig. 5A). As is the case with the *GL2* promoter (Hung et al., 1998), the *HDG2* promoter was found to drive GUS expression in the hairless cell files of the hypocotyl epidermis (Fig. 5, B and C), in which stomatal differentiation is repressed. In addition, both *HDG2* and *HDG5* promoters drove GUS expression in shoot apical meristems with higher levels in L1 cells, the epidermal layer of young leaves including trichomes, stipules, and later in stomatal meristemoids (Fig. 5, D–M). The *HDG7-GUS* plants showed a unique

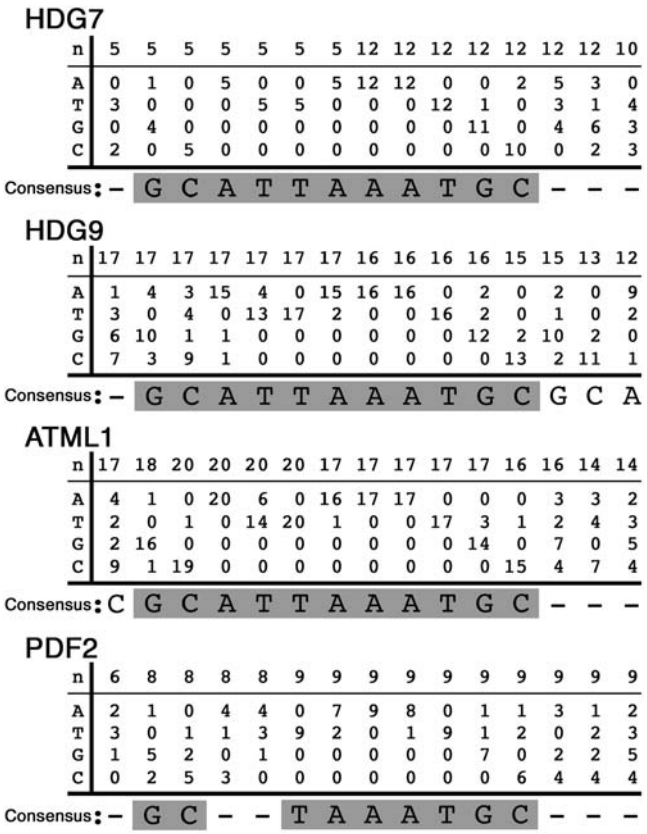

Figure 3. Determination of the consensus binding sequences for the HD-ZIP IV proteins using PCR-assisted random oligonucleotide selection. The sequences selected by MBP fusion proteins with ML1, HDG7, HDG9, and PDF2 were aligned and tabulated. The number of occurrences of the four bases and the derived consensus sequences are shown. n, The total number of oligonucleotides that are derived from random sequence positions.

GUS expression pattern in a band of cells around the base of leaf primordia (Fig. 5N), which is reminiscent of that of the *LATERAL ORGAN BOUNDARIES* gene (Shuai et al., 2002). The sections revealed that the GUS activity was localized in the outermost two or three cell layers along the boundary between two leaf primordia (Fig. 5, O and P). Plants harboring *HDG11* and *HDG12* fusions displayed GUS staining patterns similar to those observed for *HDG2* and *HDG5* fusions in apical meristems, young epidermal tissue including trichomes, and stipules (Fig. 5, Q–X). GUS expression was also detected in the epidermal cell lines along the cotyledon margin in *HDG11-GUS* seedlings (Fig. 5Q). Plants harboring *HDG8*, *HDG9*, and *HDG10* fusions showed no GUS activity in vegetative shoot tissue (data not shown).

In the root tissue, the *HDG1* promoter drove weak GUS expression in two endodermal cell lines around emergent lateral roots (Fig. 6A). *HDG2-GUS* expression was observed in primary root tips (Fig. 6B). *HDG7-GUS* expression was observed in lateral root primordia (Fig. 6, C and D) and persisted at lateral root tips (Fig. 6E). Both *HDG11* and *HDG12* promoters drove GUS expression only in lateral root tips (Fig. 6, F and G). Plants harboring *HDG5*, *HDG8*, *HDG9*, and *HDG10* fusions showed no GUS activity in roots (data not shown).

During flower development, *HDG1-GUS* expression was detectable exclusively in the epidermal layer of the stamen filament (Fig. 7, A and B). Both *HDG2* and *HDG5* promoters drove GUS expression in apical inflorescence meristems and early flower primordia, with the highest signal in the L1, and later in the carpel epidermis and ovule primordia (Fig. 7, C–I).

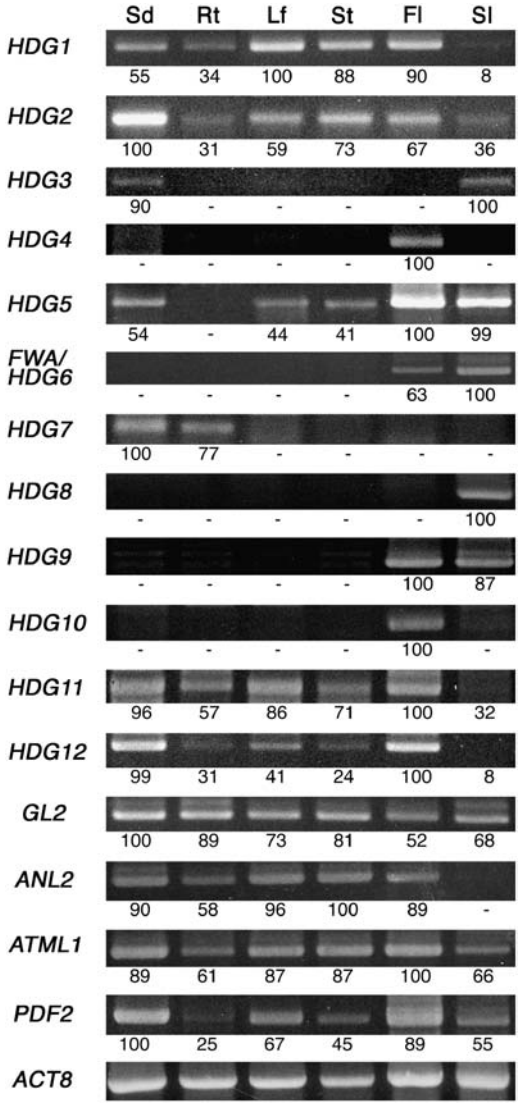

Figure 4. RT-PCR analysis of the *HDG* transcript levels in different organs. Total RNA was extracted from 7-d-old seedlings (Sd), roots of 14-d-old seedlings grown on Murashige and Skoog agar medium (Rt), leaves (Lf), stems (St), flowers (Fl), and siliques (Sl). The latter four organ samples were prepared from 40-d-old flowering plants. Values below the gel represent the ratio of each transcript to *ACT8*, with the maximum value set to 100.

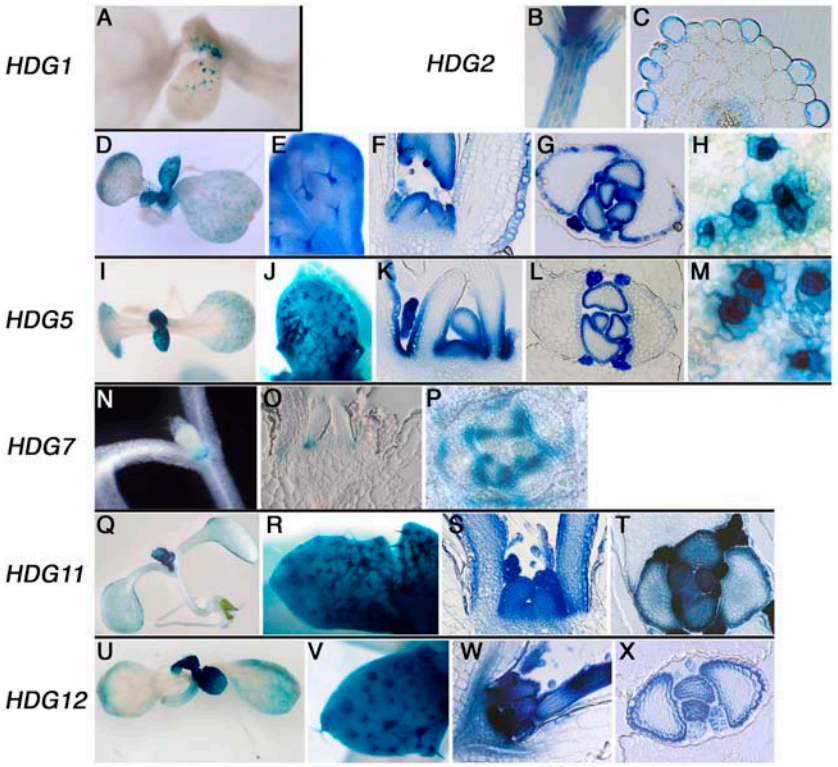

Figure 5. GUS expression patterns in the seedlings of *HDG* promoter-*GUS* transgenic lines. A, *HDG1-GUS* expression in developing trichomes. B to H, *HDG2-GUS* expression in the root hairless cell file of hypocotyls (B and C), developing leaves (D), trichomes (E), shoot apical meristems, leaf primordia, stipules (F and G), and stomatal meristemoids (H). I to M, *HDG5-GUS* expression in developing leaves (I), trichomes (J), shoot apical meristems, leaf primordia, stipules (K and L), and stomatal meristemoids (M). N to P, *HDG7-GUS* expression at the base of leaf primordia. Q to T, *HDG11-GUS* expression in cotyledon margins and developing leaves (Q), trichomes (R), shoot apical meristems, leaf primordia, and stipules (S and T). U to X, *HDG12-GUS* expression in developing leaves (U), trichomes (V), shoot apical meristems, leaf primordia, and stipules (W and X). A transverse section through hypocotyls (C) was prepared from a 5-d-old seedling of the *HDG2-GUS* line. Longitudinal sections (F, K, O, S, and W) and transverse sections (G, L, P, T, and X) through shoot apices were prepared from 5- to 7-d-old seedlings of respective plant lines.

HDG5-GUS expression was also detected in the epidermis of the stamen filament (Fig. 7G) and remarkably in stomatal guard cells of the carpel (Fig. 7J). In plants with *HDG9* and *HDG10* fusions, GUS expression was detectable exclusively in anthers, with higher activity evident in the tapetum and pollen grains (Fig. 7, K–N). Plants harboring *HDG11* and *HDG12* fusions showed GUS expression predominantly in the L1 of apical inflorescence meristems and early flower primordia, and later in the carpel epidermis and ovule primordia, patterns similar to those of *HDG2* and *HDG5* fusions (Fig. 7, O–U). GUS signals were also detectable in the stigma papillae of both *HDG11-GUS* and *HDG12-GUS* plants, the petal epidermis of *HDG11-GUS* plants, and the epidermis of the stamen filament of *HDG12-GUS* plants (Fig. 7, P–R, and T). The GUS signal in ovule primordia in plants with *HDG2*, *HDG5*, *HDG11*, and *HDG12* fusions was later confined to the nucellus (Fig. 7, R and U; data not shown).

During embryo sac formation, *HDG2-GUS* expression was restricted sharply to the chalazal end (Fig. 8, A and B). The GUS signal then extended through the endosperm (Fig. 8, C and D) and was additionally detected in the seed coat and throughout the arising embryo (Fig. 8, E and F). *HDG5-GUS* plants showed similar patterns of GUS expression to those of *HDG2-GUS* plants, except for the seed coat (Fig. 8, G–I). In plants harboring the *HDG7* fusion, weak GUS signal was initially detectable in the apical region of the heart-stage embryo (Fig. 8J) and was localized to epidermal boundaries of two cotyledons (Fig. 8, K and L). *HDG8-GUS* expression was limited to the endosperm and the whole embryo at early stages (Fig. 8, M and N), whereas *HDG9-GUS* expression was acutely limited to the chalazal end of the embryo sac (Fig. 8O). In plants with *HDG11* and *HDG12* fusions, GUS activity was detectable throughout the embryo but not in the endosperm (Fig. 8, P–S). In summary, the observed GUS patterns are in agreement with the results of RT-PCR experiments.

Phenotypes of T-DNA Insertion Mutants of the Arabidopsis HD-ZIP IV Genes

For functional analysis of the HD-ZIP IV family, T-DNA insertion mutants of all *HDG* genes, except for *HDG7*, were obtained from the SALK Institute, Syngenta or University of Wisconsin T-DNA insertion collections (Fig. 2; see ''Materials and Methods''). The *hdg7-1* allele was isolated by screening a pool of T-DNA insertion lines, which had been generated as described previously (Nakazawa et al., 2001). Homozygous mutant plants were identified by PCR genotyping using gene-specific primers (Supplemental Table I). However, all of the single mutant alleles except for *hdg11-1* and *hdg11-2* showed no discernible phenotypes as to growth and development. *hdg11-1* and *hdg11-2* appeared to have more branched trichomes compared with the wild type (Fig. 9; Table II). *hdg11-1* was crossed to *hdg12-2* to generate double mutants of these paralogous genes. Although *hdg12-2* has normal trichomes, *hdg11-1 hdg12-2* plants showed

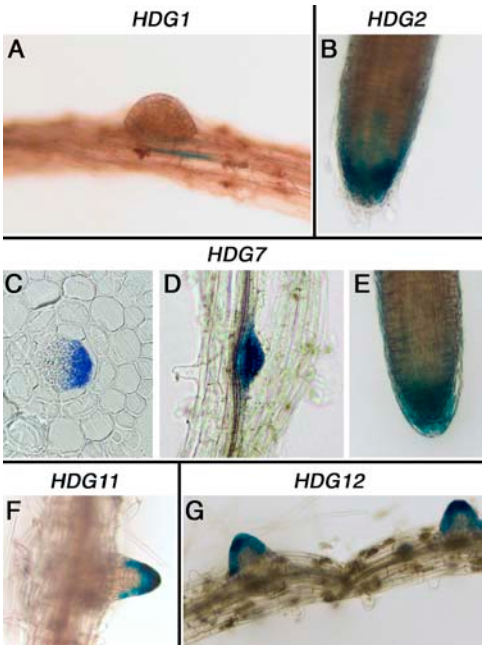

Figure 6. GUS expression patterns in the root tissue of *HDG* promoter-*GUS* transgenic lines. A, *HDG1-GUS* expression in two cell lines at the edge of emergent lateral roots. B, *HDG2-GUS* expression in primary root tips. C to E, *HDG7-GUS* expression in lateral root primordia, shown by a transverse section of primary roots (C), emerging lateral root tips (D), and primary root tips (E). F, *HDG11-GUS* expression in emerging lateral root tips. G, *HDG12-GUS* expression in emerging lateral root tips.

obvious enhancement of the excess branching phenotype of the *hdg11-1* trichome (Fig. 9; Table II). These alleles were also crossed with *gl2-t1*, which exhibits the known *gl2* phenotype in trichomes and root hairs. The *gl2* phenotype was not altered in *hdg11-1 gl2-t1*, *hdg11-2 gl2-t1*, and *hdg12-2 gl2-t1* double mutants (Fig. 9, E and F; data not shown).

We also constructed double mutants of other paralogous gene pairs, *HDG1-ANL2*, *HDG2-HDG3*, *HDG4-HDG5*, *FWA/HDG6-HDG7*, and *HDG8-HDG9*, but none of the *hdg2-3 hdg3-1*, *hdg4-1 hdg5-1*, *fwa-t1 hdg7-1*, *hdg8-1 hdg9-1*, or *hdg8-1 hdg9-2* mutants displayed an abnormal phenotype (Fig. 10A; data not shown). *hdg1-2 anl2-t1* showed no additional phenotypes to those reported for *anl2* (Kubo et al., 1999). Further double mutant analyses revealed no abnormalities in *hdg2-3 atml1-1*, *hdg2-3 pdf2-1*, *hdg2-3 hdg5-1*, and *hdg9-2 hdg10-1*. On the other hand, *hdg3-1 atml1-1* and *hdg3-1 pdf2-1* were found to have defects in cotyledon development. *hdg3-1 atml1-1* seedlings frequently (69%) exhibited hyponastic growth of cotyledons (Fig. 10B), whereas *hdg3-1 pdf2-1* seedlings showed various abnormalities including aberrant morphology (72%), cotyledon fusion (13%), no cotyledons (10%), and adventitious shoot formation on cotyledons (1%; Fig. 10, C–H). Sections of these adventitious shoots showed that they may be originated from the cotyledon epidermis of *hdg3-1 pdf2-1* seedlings (Fig. 10I).

DISCUSSION

Expression Regulation

Our results of the GUS expression patterns in transgenic Arabidopsis plants revealed that the promoters of *HDG1*, *HDG2*, *HDG5*, *HDG7*, *HDG11*, and *HDG12* preferentially direct expression in the epidermal layer of shoot organs. Because *HDG2* and *HDG5* have an L1 box motif within the 0.2-kb upstream region of the 5′ end of their full-length transcripts (data not shown), these two genes might be regulated via a feedback and/or hierarchical control through the binding of their own and/or other HD-ZIP IV proteins to the L1 box, as previously suggested for *ATML1* and *PDF2* (Abe et al., 2003).

Expression profiles of *HDG1*, *HDG2*, *HDG5*, *HDG11*, and *HDG12* reporter constructs in trichomes are reminiscent of *GL2* expression (Szymanski et al., 1998). The *GL2* promoter may be a target of transcription complexes containing the MYB protein GL1 and the basic helix-loop-helix protein GL3, although the exact binding sites for these factors have not been determined. In addition, because putative MYB binding site motifs (Sablowski et al., 1994) are present in each of these *HDG* promoter regions (data not shown), it is possible that expression of the HD-ZIP IV members in trichomes commonly involves the GL1/GL3 regulatory module. Unlike these *HDG* genes, however, *GL2* expression is also detectable in all of the cell layers of the developing leaves (Szymanski et al., 1998). Thus, it is also possible that the expression of *GL2* in trichomes is uniquely regulated by the GL1/GL3 complex, whereas the control of the other HD-ZIP IV members may result from their expression in the meristem L1.

It is noteworthy that *HDG2*, *HDG5*, and *HDG9* gene promoters drove GUS expression in the chalazal end of the embryo sac, probably representing three antipodal cells. In contrast to two synergid cells, which are adjacent to the egg cell and function in attracting a pollen tube during double fertilization (Higashiyama et al., 2001), the function of the antipodal cells, which generally degenerate no later than fertilization, remains unexplored. The availability of these *HDG* promoters that can direct cell-type-specific expression in the embryo sac should thus be an invaluable tool in the study of the genetic control of embryo sac formation and the function of its cells during fertilization.

After fertilization, *HDG2*, *HDG5*, and *HDG8* promoters resulted in GUS expression in the endosperm. We note, in terms of L1 cell specification, that the endosperm is the environment that is first encountered by an embryo and could provide the external signal required for the establishment of the embryonic protoderm. The maize *CRINKLY4* (*CR4*) gene, which encodes a receptor kinase, affects cell differentiation in the aleurone of the endosperm and in the leaf epidermis (Becraft et al., 1996). The Arabidopsis homolog of this gene, *ACR4*, has been implicated in maintaining L1 cell integrity by receiving and transmitting

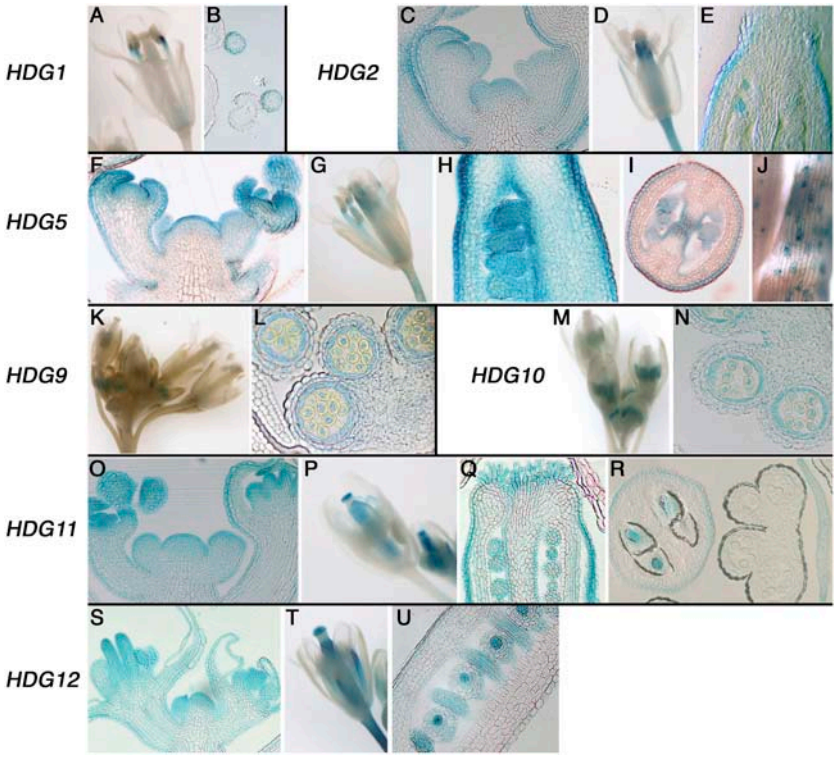

Figure 7. GUS expression patterns in the flowers of *HDG* promoter-*GUS* transgenic lines. A and B, *HDG1-GUS* expression in filaments. C to E, *HDG2-GUS* expression in inflorescence meristems (C), carpels (D and E), and ovules (E). F to J, *HDG5-GUS* expression in inflorescence meristems (F), filaments (G), carpels (G–J), and ovules (H and I). K and L, *HDG9-GUS* expression in anthers. M and N, *HDG10-GUS* expression in anthers. O to R, *HDG11-GUS* expression in inflorescence meristems (O), stigma (P and Q), petals (P and R), carpels (P–R), and ovules (Q and R). S to U, *HDG12-GUS* expression in inflorescence meristems (S), stigma (S and T), filaments (T), carpels (T and U), and ovules (U). Transverse sections (B, I, L, N, and R) and longitudinal sections (E, H, Q, and U) through floral organs were prepared from open flowers. Longitudinal sections through inflorescence apices (C, F, O, and S) were prepared from 30-d-old plants of the respective lines.

extracellular signals (Gifford et al., 2003; Watanabe et al., 2004), although the ligands for the CR4 class receptor kinases remain to be identified. *ACR4* expression is down-regulated in *atml1-1 pdf2-1* double mutants (Abe et al., 2003). Furthermore, a study of the Arabidopsis *abnormal leaf shape1* (*ale1*) mutant suggests that ALE1, a putative subtilisin-like Ser protease, functions in the separation of the endosperm from the embryo and in preventing organ fusion (Tanaka et al., 2001). Recently, the Arabidopsis *DEK1* gene, encoding a calpain-like Cys proteinase, was also shown to be a key component of the embryonic L1 cell specification pathway and to be expressed throughout the endosperm and the embryo (Johnson et al., 2005; Lid et al., 2005). The *dek1* mutant partially lacks the aleurone-like peripheral cell layer of the endosperm and also a defined protoderm of the embryo, which eventually arrests at the globular stage. The targets of ALE1 and DEK1 and the genetic relationship between these proteinases and the CR4 class

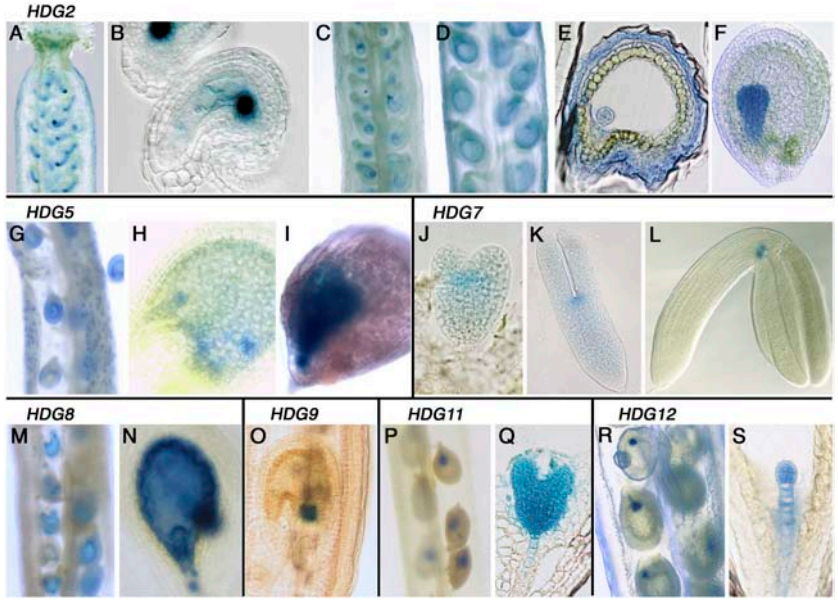

Figure 8. GUS expression patterns during embryo development of *HDG* promoter-*GUS* transgenic lines. A to F, *HDG2-GUS* expression in the chalazal end of the embryo sac (A and B), endosperms (C and D), seed coats (E), and embryos (E and F). G to I, *HDG5-GUS* expression in endosperms (G and H) and embryos (H and I). J to L, *HDG7-GUS* expression in epidermal boundaries of two cotyledons of embryos. M and N, *HDG8-GUS* expression in endosperms and embryos. O, *HDG9-GUS* expression in the chalazal end of the embryo sac. P and Q, *HDG11-GUS* expression in embryos. R and S, *HDG12-GUS* expression in embryos.

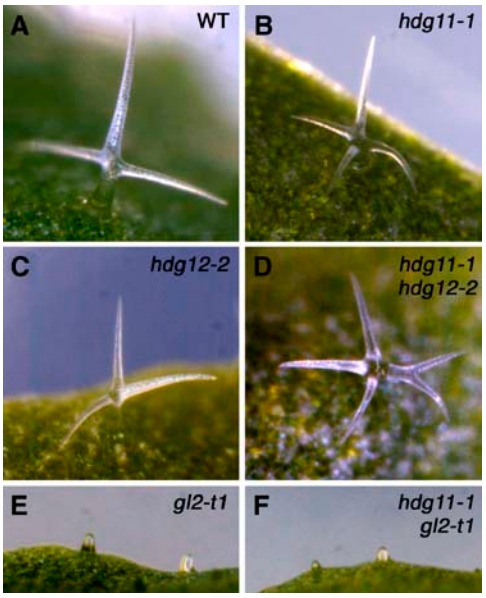

Figure 9. *HDG11* and *HDG12* act in the regulation of branching of the trichome. Typical examples of the trichome on the third leaf of 15-d-old wild-type (A), *hdg11-1* (B), *hdg12-2* (C), *hdg11-1 hdg12-2* (D), *gl2-t1* (E), and *hdg11-1 gl2-t1* (F) seedlings are shown. The excess branching of the trichome in *hdg11-1* is enhanced in *hdg11-1 hdg12-2*.

receptor kinases remain unknown. It is of interest, however, to speculate that specification of the embryonic L1 cell identity involves endosperm-derived signals whose expression might also be regulated by HD-ZIP IV transcription factors.

Some of the known HD-ZIP IV genes in gymnosperms and angiosperms contain a highly conserved 17-nucleotide-long motif, (U/A) GGUU CGGG(U/A) AUUGA CU, within their 3′-untranslated region (Ingouff et al., 2003). This motif is also present in *ATML1*, *PDF2*, *ANL2*, *HDG1*, *HDG2*, *HDG3*, *HDG4*, *HDG5*, and *HDG12* (Ingouff et al., 2003; data not shown). Although the significance of this motif in mRNA translation and stability remains to be addressed, our inability to detect GUS expression in plants with *HDG3* and *HDG4* fusions might be attributed to the absence of this motif within the fusion constructs. On the other hand, it is now well known that posttranscriptional control of the HD-ZIP III genes by their corresponding microRNA plays a key role in the regulation of stem cell maintenance and organ polarity (for review, see Bowman, 2004). MicroRNA sequences corresponding to HD-ZIP IV transcripts have not been found so far either in the literature or the current databases.

Loss-of-Function Mutants

Most of the homozygous T-DNA insertion mutants that we examined in this study display a phenotype that is indistinguishable from wild type during growth under normal conditions. We confirmed by RT-PCR experiments that each of the homozygous alleles except for *hdg2-1* and *hdg12-1* do not express full-length transcripts from the gene carrying the T-DNA insertion (Supplemental Fig. 2). It is possible, however, that the mutations used in this study do not necessarily represent null alleles. To examine whether another possibility would be that there is functional redundancy between duplicated genes, we constructed double mutants of the putative paralogous gene pairs. However, we observed no effects of the double mutant combinations of *hdg1 anl2*, *hdg2 hdg3*, *hdg4 hdg5*, *fwa/hdg6 hdg7*, and *hdg8 hdg9* upon the morphological phenotype. Even *hdg2-3 hdg3-1*, which carries an insertion within each of the *HDG2* and *HDG3* HD-coding sequences (Fig. 2), and therefore most likely represents a double complete loss-of-function mutant, displayed no visible phenotype. Furthermore, expression analyses by RT-PCR and promoter-GUS fusions revealed both overlapping and distinct expression patterns of these paralogous genes. Whereas *HDG3* expression was detected only in siliques and germinating seedlings, *HDG2* was expressed in all of the organs examined and showed a unique promoter-GUS expression pattern in stomatal meristemoids and during ovule development, similar to nonparalogous *HDG5* (Figs. 5 and 8). Endosperm-specific expression of *FWA/HDG6* (Kinoshita et al., 2004) was not shared by its paralogous gene *HDG7*, but was found to be similar to *HDG8* (Fig. 8). These results suggest that some paralogs in the HD-ZIP IV family no longer have overlapping functions and raise the possibility that the nonparalogous members in fact possess conserved functions.

HDG11 is one of the HD-ZIP IV family members for which single mutants display an abnormal phenotype. The excess branching phenotype of the trichome in *hdg11-1* is enhanced by *hdg12-2*, suggesting that both *HDG11* and *HDG12* act in repressing the outgrowth of trichomes. The lack of a trichome phenotype in *hdg12* mutants, however, suggests a subsidiary function for *HDG12* in this process or possibly an epistatic relationship between *HDG11* and *HDG12* during branch repression. Because of the *gl2* phenotype observed in *gl2 hdg11* and *gl2 hdg12* double mutants, *GL2* appears to be epistatic to *HDG11* and *HDG12*. According to genetic mapping data (Perazza et al., 1999), none of the known mutants with supernumerary branched trichomes, including *triptychon*, *kaktus*, *spindly*, *polycomb*, and *rastifari*, appear to represent an allele of *HDG11* or

Table II. *Distribution of branch point numbers of the trichome*

Genotype	No. of Branch Points[a]						
	0	1	2	3	4	5	6
Wild type (Columbia-0)	0	7.6	73.7	18.1	0.6	0	0
hdg11-1	0	2.1	19.9	46.8	27.6	3.6	0
hdg11-2	0	1.7	19.3	48.7	28.6	1.7	0
hdg12-2	0	7.5	81.3	10.8	0.4	0	0
hdg11-1 hdg12-2	0	0.7	13.8	35.5	36.2	11.5	2.3

[a]Data are shown as the percent of a total of 400 trichomes, counted on the third and fourth leaves of the respective plant lines.

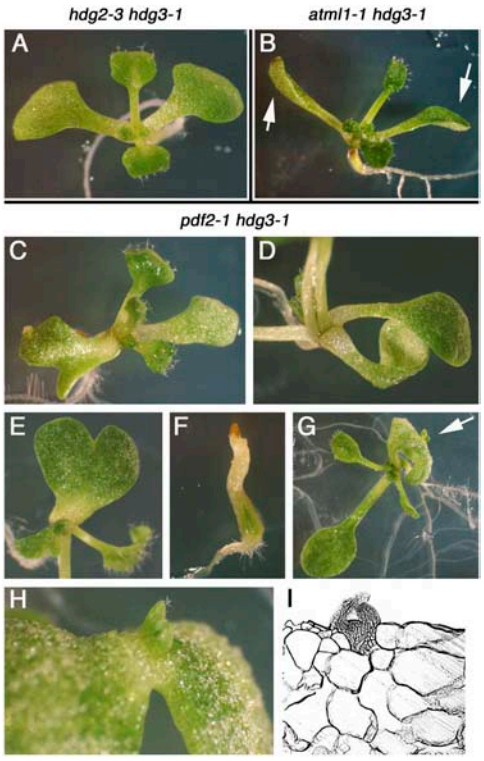

Figure 10. *HDG3* acts in the cotyledon development in cooperation with *ATML1* and *PDF2*. Ten-day-old seedlings of *hdg2-3 hdg3-1* (A), *atml1-1 hdg3-1* (B), and *pdf2-1 hdg3-1* (C–I) are shown. Hyponasty of *atml1-1 hdg3-1* cotyledons is indicated by arrows in B. *pdf2-1 hdg3-1* mutants exhibit a variety of morphological defects in cotyledons such as altered form (C), nonopposite arrangement (D), cotyledon fusion (E), pin (F), and adventitious shoot formation (G). H and I are a magnified view and a section of the adventitious shoot shown by an arrow in G, respectively.

HDG12. These mutants have been shown to undergo extra rounds of DNA endoreduplication, suggesting a link between this and trichome branching (Hülskamp et al., 1994), but it remains to be determined whether the endoreduplication levels of the trichome are affected in mutant alleles of *HDG11* and *HDG12*. In any case, further studies with these alleles, such as the analysis of genetic interactions with reduced trichome branching mutations (Luo and Oppenheimer, 1999) and a search for the target genes regulated by *HDG11* and *HDG12*, should provide further clues to elucidate the regulatory network of trichome branch formation.

The cotyledon phenotypes observed in *pdf2 hdg3* and *atml1 hdg3* are consistent with the *HDG3* expression limited to germinating seedlings and siliques containing developing embryos and suggest that, in combination with *PDF2* and *ATML1*, *HDG3* likely acts in epidermal cell differentiation in cotyledon development. The apparent difference of the phenotype between *pdf2 hdg3* and *atml1 hdg3* might imply functional differences between *PDF2* and *ATML1*, which have not yet been noted. To further address the function of each gene, however, it will be necessary to construct multiple mutant combinations, based on the similarity of expression patterns of the members, and this is currently under way in our laboratory.

Binding Sequences

The results of HD binding site selection experiments using HDG7, HDG9, ATML1, and PDF2 recombinant proteins revealed a 5′-GCATTAAATGC-3′ consensus sequence (Fig. 3). This sequence is overlapping with the L1 box sequence 5′-TAAATG(C/T)A-3′ (Abe et al., 2001). It is also consistent with the sequence 5′-CATT(A/T)AATG-3′, which was identified as a preferential target of the sunflower (*Helianthus annuus*) HD-ZIP IV protein HAHR1 (Tron et al., 2001). According to earlier in vitro studies, HD-ZIP I proteins bind the pseudopalindromic sequence 5′-CAAT(A/T)ATTG-3′, whereas HD-ZIP II proteins bind the sequence 5′-CAAT(G/C)ATTG-3′ (Sessa et al., 1993; Palena et al., 1999). HD-ZIP III proteins were shown to bind the extended sequence 5′-GTAAT(G/C)ATTAC-3′ (Sessa et al., 1998). Taken together, the sequences targeted by HD-ZIP IV proteins may be characterized by the motif 5′-TAAA-3′, which is also present in a target site of GL2 within the phospholipase Dζ1 gene promoter (Ohashi et al., 2003). Interestingly, amino acid substitutions of both I47F and A54T, within the HD of a sunflower HD-ZIP I protein HAHB4, results in the same binding behavior as HAHR1, suggesting a critical role for the residues at positions 47 and 54 in DNA sequence recognition (Tron et al., 2001). As shown in Figure 1B, two residues, F47 and T54, among the four DNA recognition residues within the helix III region are specifically conserved in all HDG proteins except FWA/HDG6. The other two residues, Q50 and N51, are common beyond these classes and occur in most of the animal HD proteins (for review, see Gehring et al., 1994).

It should be emphasized that the DNA-binding activity of the HD-ZIP IV proteins can be altered by physiological conditions. These proteins contain two conserved Cyss within a loop that truncates a ZIP-like dimerization motif. Redox conditions have been shown to cause a significant increase in DNA binding by monomer formation of the sunflower HAHR1 (Tron et al., 2002). It is also likely that preferential binding sequences for HD-ZIP IV members are altered by combinatorial interactions between the members to form homo- or heterodimers through their ZIP motif. In addition, the presence of the START domain in HD-ZIP III and HD-ZIP IV proteins implies the involvement of lipid/sterol binding in their activation, although the underlying molecular mechanism is unknown. Thus, we cannot exclude the possibility that the preferential target motif identified in this study does not represent the bona fide DNA-binding sequences of each HDG protein.

CONCLUSION

In this study we set about providing a comprehensive characterization of the HD-ZIP IV family in

Arabidopsis. The multiplicity of the members and the lack of abnormal phenotypes for the mutants examined, except for *hdg11* alleles, suggest functional redundancy among the members. This could be further assessed by constructing multiple mutants and/or by making transgenic plants with chimeric HDG fusions with either the herpes simplex virus VP16 activation domain (Ohashi et al., 2003) or the Drosophila Engrailed repressor domain (Khaled et al., 2005). HD-ZIP I, II, and III gene sequences are highly conserved from moss to seed plants (Sakakibara et al., 2001, 2003; Floyd et al., 2006). Furthermore, the presence of multiple genes of the HD-ZIP IV family in the EST database of *P. patens* (http://moss.nibb.ac.jp/) indicates that the origin of all HD-ZIP families precedes the divergence of bryophytes and vascular plants. Genetic analysis of these genes in the moss, which has single-cell-layered leaf-like organs, will thus be fundamental to the elucidation of roles for the respective family members and will help to determine whether these genes have retained similar functions during evolution.

MATERIALS AND METHODS

Plant Material and Growth Conditions

The wild-type Arabidopsis (*Arabidopsis thaliana*) plants used in this study were of the Columbia-0 ecotype. T-DNA insertion alleles *hdg1-1* (SALK_006757), *hdg1-2* (SALK_062171), *hdg2-2* (SALK_27828), *hdg2-3* (SALK_138646), *hdg3-1* (SALK_033462), *hdg5-1* (SALK_032993), *hdg9-2* (SALK_079210), *hdg10-1* (SALK_116071), *hdg11-2* (SALK_044434), *hdg12-2* (SALK_127261), *fwa-t1* (SALK_064256), *gl2-t1* (SALK_030214), and *anl2-t1* (SALK_000196) were derived from the Salk Institute Genomic Analysis Laboratory T-DNA insertion lines (http://signal.salk.edu). *hdg4-1* (WiscDsLox382F6) was derived from the knockout facility at the University of Wisconsin (Sussman et al., 2000). All of these alleles were obtained from the Arabidopsis Biological Resource Center (Ohio State University, Columbus, Ohio). The *hdg8-1* (SAIL_586 E12), *hdg9-1* (SAIL_634 D06), *hdg11-1* (SAIL_865 G09), and *hdg12-1* (SAIL_870 c06) alleles were obtained from the Syngenta T-DNA insertion collection (www.tmri.org). The *hdg7-1* allele was isolated by screening a population of T-DNA insertion lines that had been generated as previously described (Nakazawa et al., 2001). The primers used in the screening were a *HDG7*-specific primer, HDG7-1F (Supplemental Table I), and a T-DNA left border primer, NY-LB (5′-ATAAC GCTGC GGACA TCTAC-3′). Isolation of the *atml1-1* and *pdf2-1* alleles has been described previously (Abe et al., 2003).

Plants were grown on rock-wool bricks supplemented with vermiculite in growth chambers or in petri dishes, with medium containing 0.8% agar, 3% Suc, and Murashige and Skoog salts (pH 5.7; Wako). The cultures were incubated at 22°C under continuous light after surface sterilization of seeds.

Genotyping

The genotype of each T-DNA insertion allele was determined by PCR of genomic DNA with the gene-specific primers shown in Supplemental Table I and Abe et al. (2003). The conditions for the PCR reactions were: 50 cycles of 30 s at 94°C, 30 s at 55°C, and 120 s at 72°C.

RT-PCR

Total RNA was extracted from frozen tissues by the SDS-phenol method, precipitated with 2 M LiCl, and treated with RNase-free DNaseI (Takara). First-strand cDNA synthesis was carried out using 1 μg of total RNA with an oligo dT primer according to the protocols of the RNA PCR kit (Takara). Primers used in the amplifications and the sizes of RT-PCR products are shown in Supplemental Table I and Abe et al. (2003). Primers for *ACTIN8* (*ACT8*; At1g49240), which were used in control reactions, were ACT8F (5′-GTGAG CCAGA TCTTC ATCGT C-3′) and ACT8R (5′-TCTCT TGCTC GTAGT CGACA G-3′). PCR parameters were 30 (*HDG1*, *HDG2*, *HDG11*, *HDG12*, *GL2*, *ANL2*, *ATML1*, *PDF2*, and *ACT8*), 40 (*HDG5*, *HDG8*, *HDG9*, and *HDG10*), or 45 (*HDG3*, *HDG4*, *FWA/HDG6*, and *HDG7*) cycles of 30 s at 94°C, 30 s at 55°C, and 120 s at 72°C. The PCR products were separated on a 1.5% agarose gels that were stained with ethidium bromide and quantified densitometrically.

PCR-Assisted Binding Site Selection

For the MBP-HDG7 fusion constructs, the full-length *HDG7* cDNA sequence was amplified by RT-PCR with the primers H7F (5′-GAATT CAGAG GGAAA ATGAA TGGCG-3′) and H7R (5′-ACTAG TCCTA CAACT TTAGC TAAGC-3′). The underlined sequences indicate the addition of restriction sites to the primer sequence. The amplified PCR products were digested with *Eco*RI and *Spe*I, and subcloned into the pMAL-c2 vector (New England Biolabs). For the MBP-HDG9 fusion construct, the full-length *HDG9* cDNA sequence was amplified by RT-PCR with HDG9-2F and HDG9-1R primers (Supplemental Table I). The amplified PCR products were then cloned into the pGEM-T Easy vector and subcloned into pMAL-c2 using *Eco*RI and *Spe*I restriction sites. The MBP-ATML1 and MBP-PDF2 constructs have been previously described (Abe et al., 2003).

The MBP fusion constructs were introduced into the *Escherichia coli* strain BL-21 and the transformed bacteria were cultured at 30°C in Luria-Bertani medium, containing 0.2% Glc and 50 μg mL^{-1} ampicillin, until they reached OD_{600} values of about 0.5. Isopropylthio-β-galactoside was then added to the cultures at a final concentration of 0.1 mM. Crude extracts for binding selection were prepared according to the manufacturer's instructions and the protein concentration was estimated using the Bradford assay kit (Bio-Rad).

The selection of binding sequences for the MBP fusion proteins was performed according to the method of Pierrou et al. (1995). The double-stranded random DNA molecules were synthesized from template oligonucleotides [5′-CGACC ATCAT TCGCA GTT$(N)_{20}$C AGCTC CAGTT TCCGT TG-3′] and the reverse primer 5′-AACAA CGGAA ACTGG AGCTG-3′ in a single cycle of 3 min at 95°C, 30 min at 60°C, and 10 min at 72°C. Ten micrograms of random DNA was then mixed with 1 μL of bacterial crude extracts, containing fusion proteins in 100 μL of the binding buffer [20 mM HEPES/KOH pH 7.9, 50 mM KCl, 2 mM $MgCl_2$, 0.5 mM EDTA, 10% glycerol, 1 mg mL^{-1} bovine serum albumin, 2 mM dithiothreitol, and 10 mg mL^{-1} poly(dI/dC)] and incubated for 30 min at room temperature. After the first incubation, amylose resin (10% slurry in the binding buffer) was added and incubated by gently shaking for 1 h on ice. The MBP fusion proteins bound to the amylose resin were pelleted by centrifugation, washed five times with the binding buffer, and resuspended in 120 μL distilled water. Samples were boiled for 10 min to elute bound DNA. After centrifugation, 70 μL of the supernatant was used as a template for PCR with the forward primer 5′-ATCGA CCATC ATTCG CAGTT-3′ and reverse primers. The conditions for PCR in this case were: 5 min at 96°C and 20 cycles of 30 s at 96°C, 30 s at 56°C, and 20 s at 72°C. The PCR products were then extracted with phenol/chloroform, precipitated with ethanol, and resuspended in distilled water. Half volumes of the purified PCR products were subsequently used for the next cycle of selection. After the fifth round of selection, the selected DNA fragments were cloned into the pGEM-T Easy vector and sequenced.

T-DNA Construction and Plant Transformation

The PCR primers used to clone promoter fragments of each gene were shown in Supplemental Table II. All of the PCR fragments were cloned into the pGEM-T Easy Vector (Promega) and subsequently inserted in front of the GUS gene in the binary vector pBI101.2 (CLONTECH) by using the restriction sites within the primers. The lengths of the promoter fragments for *HDG1-HDG12* are 1.35, 2.47, 2.25, 2.57, 2.01, 2.26, 1.54, 2.67, 2.27, 2.61, and 1.93 kb, respectively.

The T-DNA constructs were introduced into wild-type plants via Agrobacterium-mediated transformation as described previously (Clough and Bent, 1998). Transformants were isolated by kanamycin selection. For each construct, at least four independent lines that may carry a single copy of the construct were selected from T2 seeds, and their progenies homozygous for the T-DNA constructs were used for further experiments.

GUS Staining

Tissues were prefixed in ice-cold 90% (v/v) acetone for 20 min, rinsed twice with a 50 mM sodium phosphate buffer (pH 7.2) containing 0.05% Triton

X-100, 2 mM $K_3Fe(CN)_6$, and 2 mM $K_4Fe(CN)_6$, infiltrated with a staining solution (1 mM 5-bromo-4-chloro-3-indolyl-β-GlcUA in the buffer) under vacuum on ice for 10 min, and incubated at 37°C for 12 h. The stained samples were cleared by several changes of 70% (v/v) ethanol. For sections, the samples were dehydrated in a graded ethanol series from 70% to 100% and embedded in Technovit 7100 (Kulzer) according to the manufacturer's protocol. For whole-mount clearing, samples were soaked in clearing solution (chloral hydrate:water:glycerol, 8:2:1) for 2 to 8 h. Tissues or sections (8-μm thick) were then mounted on slides and examined under a light microscope.

Sequence data from this article can be found in the GenBank/EMBL data libraries under the accession numbers provided in Table I.

ACKNOWLEDGMENTS

We thank Mitsuyasu Hasebe for his comments on the manuscript. We are also grateful to the Arabidopsis Biological Resource Center and Syngenta Biotechnology for providing T-DNA insertion lines.

Received January 21, 2006; revised June 4, 2006; accepted June 6, 2006; published June 15, 2006.

LITERATURE CITED

Abe M, Katsumata H, Komeda Y, Takahashi T (2003) Regulation of shoot epidermal cell differentiation by a pair of homeodomain proteins in Arabidopsis. Development **130:** 635–643

Abe M, Takahashi T, Komeda Y (2001) Identification of a cis-regulatory element for L1 layer-specific gene expression, which is targeted by an L1-specific homeodomain protein. Plant J **26:** 487–494

Becraft PW, Stinard PS, McCarty DR (1996) CRINKLY4: a TNFR-like receptor kinase involved in maize epidermal differentiation. Science **273:** 1406–1409

Blanc G, Barakat A, Guyot R, Cooke R, Delseny M (2000) Extensive duplication and reshuffling in the Arabidopsis genome. Plant Cell **12:** 1093–1101

Bowman JL (2004) Class III HD-Zip gene regulation, the golden fleece of ARGONAUTE activity? Bioessays **26:** 938–942

Clough SJ, Bent AF (1998) Floral dip: a simplified method for *Agrobacterium*-mediated transformation of *Arabidopsis thaliana*. Plant J **16:** 735–743

Di Cristina M, Sessa G, Dolan L, Linstead P, Baima S, Ruberti I, Morelli G (1996) The Arabidopsis Athb-10 (GLABRA2) is an HD-Zip protein required for regulation of root hair development. Plant J **10:** 393–402

Floyd SK, Zalewski CS, Bowman JL (2006) Evolution of class III homeodomain-leucine zipper genes in streptophytes. Genetics **173:** 373–388

Gehring WJ, Qian YQ, Billeter M, Furukubo-Tokunaga K, Schier AF, Resendez-Perez D, Affolter M, Otting G, Wüthrich K (1994) Homeodomain-DNA recognition. Cell **78:** 211–223

Gifford ML, Dean S, Ingram GC (2003) The Arabidopsis *ACR4* gene plays a role in cell layer organisation during ovule integument and sepal margin development. Development **130:** 4249–4258

Henriksson E, Olsson AS, Johannesson H, Johansson H, Hanson J, Engstrom P, Soderman E (2005) Homeodomain leucine zipper class I genes in Arabidopsis: expression patterns and phylogenetic relationships. Plant Physiol **139:** 509–518

Higashiyama T, Yabe S, Sasaki N, Nishimura Y, Miyagishima S, Kuroiwa H, Kuroiwa T (2001) Pollen tube attraction by the synergid cell. Science **293:** 1480–1483

Hülskamp M, Misra S, Jurgens G (1994) Genetic dissection of trichome cell development in Arabidopsis. Cell **76:** 555–566

Hung CY, Lin Y, Zhang M, Pollock S, Marks MD, Schiefelbein J (1998) A common position-dependent mechanism controls cell-type patterning and *GLABRA2* regulation in the root and hypocotyl epidermis of Arabidopsis. Plant Physiol **117:** 73–84

Ingouff M, Farbos I, Lagercrantz U, von Arnold S (2001) *PaHB1* is an evolutionary conserved HD-GL2 homeobox gene expressed in the protoderm during Norway spruce embryo development. Genesis **30:** 220–230

Ingouff M, Farbos I, Wiweger M, von Arnold S (2003) The molecular characterization of *PaHB2*, a homeobox gene of the HD-GL2 family expressed during embryo development in Norway spruce. J Exp Bot **54:** 1343–1350

Ingram GC, Boisnard-Lorig C, Dumas C, Rogowsky PM (2000) Expression patterns of genes encoding HD-ZipIV homeodomain proteins define specific domains in maize embryos and meristems. Plant J **22:** 401–414

Ingram GC, Magnard JL, Vergne P, Dumas C, Rogowsky PM (1999) *ZmOCL1*, an HDGL2 family homeobox gene, is expressed in the outer cell layer throughout maize development. Plant Mol Biol **40:** 343–354

Ito M, Sentoku N, Nishimura A, Hong SK, Sato Y, Matsuoka M (2002) Position dependent expression of GL2-type homeobox gene, *Roc1*: significance for protoderm differentiation and radial pattern formation in early rice embryogenesis. Plant J **29:** 497–507

Johnson KL, Degnan KA, Walker JR, Ingram GC (2005) *AtDEK1* is essential for specification of embryonic epidermal cell fate. Plant J **44:** 114–127

Khaled AS, Vernoud V, Ingram GC, Perez P, Sarda X, Rogowsky PM (2005) *Engrailed-ZmOCL1* fusions cause a transient reduction of kernel size in maize. Plant Mol Biol **58:** 123–139

Kinoshita T, Miura A, Choi Y, Kinoshita Y, Cao X, Jacobsen SE, Fischer RL, Kakutani T (2004) One-way control of *FWA* imprinting in Arabidopsis endosperm by DNA methylation. Science **303:** 521–523

Kubo H, Peeters AJ, Aarts MG, Pereira A, Koornneef M (1999) *ANTHOCYANINLESS2*, a homeobox gene affecting anthocyanin distribution and root development in Arabidopsis. Plant Cell **11:** 1217–1226

Lid SE, Olsen L, Nestestog R, Aukerman M, Brown RC, Lemmon B, Mucha M, Opsahl-Sorteberg HG, Olsen OA (2005) Mutation in the *Arabidopsis thaliana DEK1* calpain gene perturbs endosperm and embryo development while over-expression affects organ development globally. Planta **221:** 339–351

Lu P, Porat R, Nadeau JA, O'Neill SD (1996) Identification of a meristem L1 layer-specific gene in Arabidopsis that is expressed during embryonic pattern formation and defines a new class of homeobox genes. Plant Cell **8:** 2155–2168

Luo D, Oppenheimer DG (1999) Genetic control of trichome branch number in Arabidopsis: the roles of the *FURCA* loci. Development **126:** 5547–5557

Masucci JD, Rerie WG, Foreman DR, Zhang M, Galway ME, Marks MD, Schiefelbein JW (1996) The homeobox gene *GLABRA2* is required for position-dependent cell differentiation in the root epidermis of *Arabidopsis thaliana*. Development **122:** 1253–1260

Nakazawa M, Yabe N, Ichikawa T, Yamamoto YY, Yoshizumi T, Hasunuma K, Matsui M (2001) *DFL1*, an auxin-responsive *GH3* gene homologue, negatively regulates shoot cell elongation and lateral root formation, and positively regulates the light response of hypocotyl length. Plant J **25:** 213–221

Ohashi Y, Oka A, Rodrigues-Pousada R, Possenti M, Ruberti I, Morelli G, Aoyama T (2003) Modulation of phospholipid signaling by GLABRA2 in root-hair pattern formation. Science **300:** 1427–1430

Palena CM, Gonzalez DH, Chan RL (1999) A monomer-dimer equilibrium modulates the interaction of the sunflower homeodomain leucine-zipper protein Hahb-4 with DNA. Biochem J **341:** 81–87

Perazza D, Herzog M, Hulskamp M, Brown S, Dorne AM, Bonneville JM (1999) Trichome cell growth in Arabidopsis thaliana can be derepressed by mutations in at least five genes. Genetics **152:** 461–476

Pierrou S, Enerback S, Carlsson P (1995) Selection of high-affinity binding sites for sequence-specific, DNA binding proteins from random sequence oligonucleotides. Anal Biochem **229:** 99–105

Ponting CP, Aravind L (1999) START: a lipid-binding domain in StAR, HD-ZIP and signalling proteins. Trends Biochem Sci **24:** 130–132

Prigge MJ, Otsuga D, Alonso JM, Ecker JR, Drews GN, Clark SE (2005) Class III homeodomain-leucine zipper gene family members have overlapping, antagonistic, and distinct roles in Arabidopsis development. Plant Cell **17:** 61–76

Rerie WG, Feldmann KA, Marks MD (1994) The *GLABRA2* gene encodes a homeodomain protein required for normal trichome development in Arabidopsis. Genes Dev **8:** 1388–1399

Ruberti I, Sessa G, Lucchetti S, Morelli G (1991) A novel class of plant proteins containing a homeodomain with a closely linked leucine zipper motif. EMBO J **10:** 1787–1791

Sablowski RWM, Moyano E, Culianez-Macia FA, Schuch W, Martin C, Bevan M (1994) A flower-specific Myb protein activates transcription of phenylpropanoid biosynthetic genes. EMBO J **13:** 128–137

Saitou N, Nei M (1987) The neighbor-joining method: a new method for reconstructing phylogenetic tree. Mol Biol Evol **4:** 406–425

Sakakibara K, Nishiyama T, Kato M, Hasebe M (2001) Isolation of homeodomain-leucine zipper genes from the moss *Physcomitrella patens* and the evolution of homeodomain-leucine zipper genes in land plants. Mol Biol Evol **18:** 491–502

Sakakibara K, Nishiyama T, Sumikawa N, Kofuji R, Murata T, Hasebe M (2003) Involvement of auxin and a homeodomain-leucine zipper I gene in rhizoid development of the moss *Physcomitrella patens*. Development **130:** 4835–4846

Schrick K, Nguyen D, Karlowski WM, Mayer KF (2004) START lipid/sterol-binding domains are amplified in plants and are predominantly associated with homeodomain transcription factors. Genome Biol **5:** R41

Sessa G, Morelli G, Ruberti I (1993) The Athb-1 and -2 HD-Zip domains homodimerize forming complexes of different DNA binding specificities. EMBO J **12:** 3507–3517

Sessa G, Steindler C, Morelli G, Ruberti I (1998) The Arabidopsis *Athb-8*, *-9* and *-14* genes are members of a small gene family coding for highly related HD-ZIP proteins. Plant Mol Biol **38:** 609–622

Sessions A, Weigel D, Yanofsky MF (1999) The *Arabidopsis thaliana MERISTEM LAYER 1* promoter specifies epidermal expression in meristems and young primordia. Plant J **20:** 259–263

Shuai B, Reynaga-Pena CG, Springer PS (2002) The lateral organ boundaries gene defines a novel, plant-specific gene family. Plant Physiol **129:** 747–761

Soppe WJ, Jacobsen SE, Alonso-Blanco C, Jackson JP, Kakutani T, Koornneef M, Peeters AJ (2000) The late flowering phenotype of *fwa* mutants is caused by gain-of-function epigenetic alleles of a homeodomain gene. Mol Cell **6:** 791–802

Sussman MR, Amasino RM, Young JC, Krysan PJ, Austin-Phillips S (2000) The Arabidopsis knockout facility at the University of Wisconsin-Madison. Plant Physiol **124:** 1465–1467

Szymanski DB, Jilk RA, Pollock SM, Marks MD (1998) Control of *GL2* expression in Arabidopsis leaves and trichomes. Development **125:** 1161–1171

Tanaka H, Onouchi H, Kondo M, Hara-Nishimura I, Nishimura M, Machida C, Machida Y (2001) A subtilisin-like serine protease is required for epidermal surface formation in Arabidopsis embryos and juvenile plants. Development **128:** 4681–4689

Tavares R, Aubourg S, Lecharny A, Kreis M (2000) Organization and structural evolution of four multigene families in *Arabidopsis thaliana*: *AtLCAD*, *AtLGT*, *AtMYST* and *AtHD-GL2*. Plant Mol Biol **42:** 703–717

Thompson JD, Higgins DG, Gibson TJ (1994) CLUSTAL W: improving the sensitivity of progressive multiple sequence alignment through sequence weighting, position-specific gap penalties and weight matrix choice. Nucleic Acids Res **22:** 4673–4680

Tron AE, Bertoncini CW, Chan RL, Gonzalez DH (2002) Redox regulation of plant homeodomain transcription factors. J Biol Chem **277:** 34800–34807

Tron AE, Bertoncini CW, Palena CM, Chan RL, Gonzalez DH (2001) Combinatorial interactions of two amino acids with a single base pair define target site specificity in plant dimeric homeodomain proteins. Nucleic Acids Res **29:** 4866–4872

Vision TJ, Brown DG, Tanksley SD (2000) The origins of genomic duplications in Arabidopsis. Science **290:** 2114–2117

Watanabe M, Tanaka H, Watanabe D, Machida C, Machida Y (2004) The ACR4 receptor-like kinase is required for surface formation of epidermis-related tissues in *Arabidopsis thaliana*. Plant J **39:** 298–308

Yang JY, Chung MC, Tu CY, Leu WM (2002) *OSTF1*: a HD-GL2 family homeobox gene is developmentally regulated during early embryogenesis in rice. Plant Cell Physiol **43:** 628–638